

Computer Vision Techniques for Quantifying, Tracking, and Identifying Bioluminescent Plankton

Donna M. Kocak, Niels da Vitoria Lobo, and Edith A. Widder

Abstract—This paper applies computer vision techniques to underwater video images of bioluminescent biota for quantifying, tracking, and identification. Active contour models are adapted for computerized image segmentation, labeling, tracking, and mapping of the bioluminescent plankton recorded by low-light-level video techniques. The system automatically identifies luminous events and extracts features such as duration, size, and coordinates of the point of impact, and uses this information to taxonomically classify the plankton species. This automatic classification can aid oceanographic researchers in characterizing the *in situ* spatial and temporal relationships of these organisms in their underwater environment. Experiments with real oceanographic data are reported. The results indicate that the approach yields performance comparable to human expert level capability. Furthermore, because the described technique has the potential to rapidly process vast quantities of video data, it may prove valuable for other similar applications.

Index Terms—Active contour models, bioluminescent plankton, computer vision tracking, undersea taxonomic classification.

I. INTRODUCTION

THIS PAPER applies computer vision techniques to underwater video images of bioluminescent biota for quantifying, tracking, and identification. The system automatically extracts characteristics such as size, duration, and the spatial coordinates of each bioluminescent emission and uses this information to taxonomically classify the plankton species. This automatic classification can aid oceanographic researchers in characterizing the *in situ* spatial and temporal relationships of these organisms in their underwater environment.

In portions of the ocean, bioluminescent organisms account for greater than 90% of the ocean's animal life [7]. Although many of them are small ($\leq 50 \mu\text{m}$), the organisms may be distinguished by the bioluminescent emissions they produce, each species having a unique flash pattern (much like fireflies). Scientists studying these creatures require information regarding their behavior, mobility, and local and global distributions. The traditional method of trawling nets from ships can only yield such gross information as the number of organisms within a sampled volume. New methods are needed to collect

and process data that reveal the spatial relationships among organisms in their natural distributions. Engineers at Harbor Branch Oceanographic Institution (HBOI) have developed a manned submersible vehicle equipped with unique data collection devices that enable researchers to observe and record the behavior of marine fauna *in situ*. Population distribution data in the form of a video sequence are collected using the equipment shown in Fig. 1. In this configuration, the submersible moves slowly (0.5 kn) and consistently through the open ocean in a horizontal direction, performing a transect. Organisms which come into contact with the 1-m-diameter transect screen are mechanically stimulated to luminesce. The flash patterns are recorded by an intensified silicon-intensified target (ISIT) video camera located directly behind the screen. An example of a video image is shown in Fig. 2. The time stamp on the bottom of each image represents hours, minutes, seconds, and frames where frames range from 0 to 29 (30 frames/s). During each horizontal transect, a quantitative plankton sample is collected by a suction sampling pump with an in-line flow meter and mesh screen at the outflow of the rotary sampling collection containers. Approximately 340 liters are pumped during each 3-min transect. These quantitative samples afford the investigator a basis for comparison and confirmation when attempting to identify species in the video data [19]–[21].

However, the sheer volume of video data recorded as described over the period of several hours makes manual analysis impractical. This paper presents a novel automated approach to tracking and identifying underwater bioluminescent organisms based on their emission patterns recorded by ISIT video. The approach uses active contour models to perform image segmentation, labeling, and tracking [9]. These models, also called snakes, are “dropped” in a grid-like pattern over each recorded video image. The snakelets (collections of small snakes [12]) that represent image features are then grouped to differentiate bioluminescent organisms from noise and background. As each sequential frame is processed, the image features are tracked by the snakelets. Characteristics such as duration, size, and coordinates of the point of impact of each emission pattern are extracted and used to identify the organism species. This information is combined to characterize the *in situ* spatial relationships of these organisms.

Manuscript received July 20, 1997; revised September 21, 1998. This work was supported by Harbor Branch Oceanographic Institution contribution number 1261.

D. M. Kocak is with the Engineering Division, Harbor Branch Oceanographic Institution, Fort Pierce, FL 34946 USA.

N. da Vitoria Lobo is with the Computer Science Department, University of Central Florida, Orlando, FL 32816 USA.

E. A. Widder is with the Marine Science Division, Harbor Branch Oceanographic Institution, Fort Pierce, FL 34946 USA.

Publisher Item Identifier S 0364-9059(99)01070-5.

II. RELATED WORK

A. Basic Snake Model

A snake or active contour model, originally defined by Kass *et al.* [9], is an energy-minimizing spline. As such, the snake

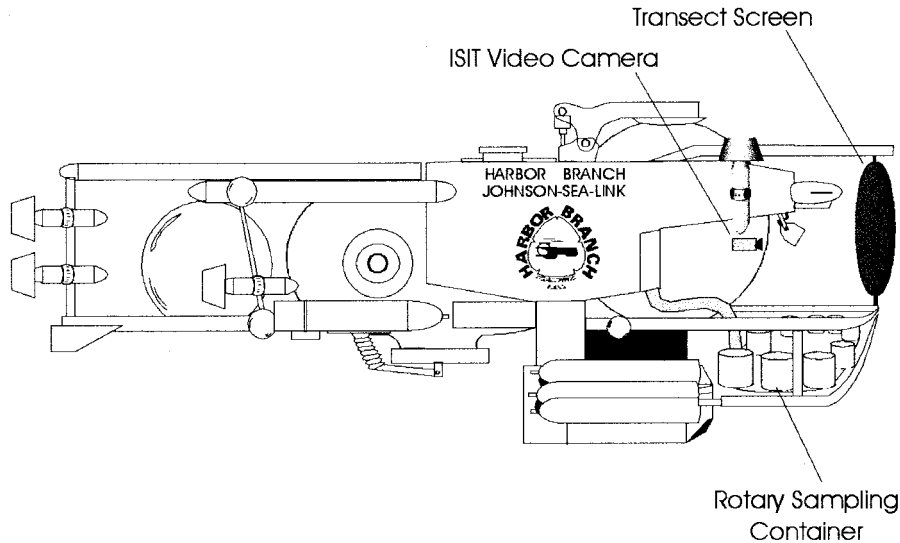


Fig. 1. Submersible equipped with sampling gear.

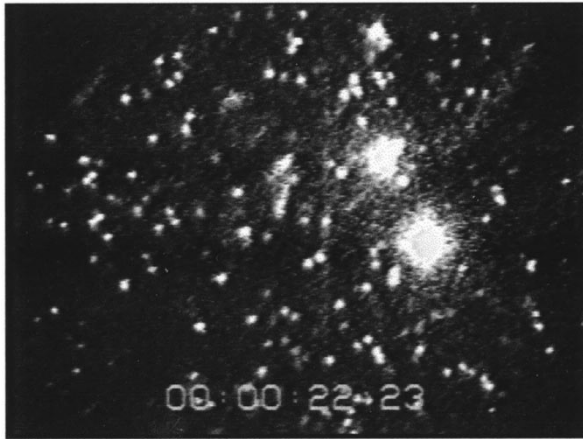


Fig. 2. Example ISIT video image showing bioluminescent emissions.

seeks a local minimum or maximum intensity area (or contour) in the image on which it is initialized through an iterative process. The physical properties (or energies) defining the snake contribute to its movement. Fig. 3 provides an example of two snakes seeking local maximas on the image pixels. In this example, snake 1 consists of three nodes. Because the neighboring pixels maintain similar intensities of those occupied by the snake nodes, the snake is unable to move and remains "stuck" at this location. However, snake 2, which consists of four nodes, is able to move toward the darker pixels along the intensity gradient. Thus, the snake will converge, or "settle," along the contour of the image object after several iterations.

Mathematically, the position of the snake is defined parametrically by

$$v(s) = (x(s), y(s)) \quad (1)$$

where s is the contour length and (x, y) is the coordinate of each node. The minimization process searches for a local minimum or maximum using energy functionals that incorporate prior knowledge of the features being sought [4]. In the basic

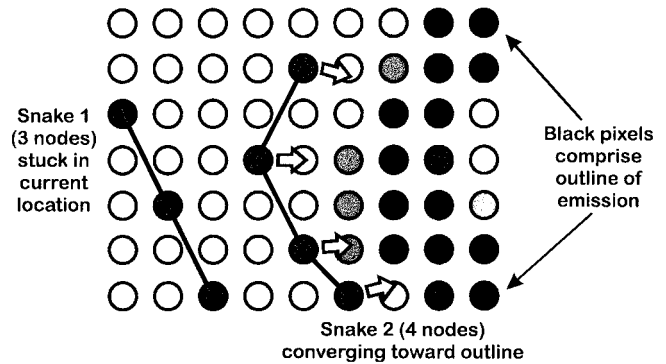


Fig. 3. Example of two snake models minimizing on a pixel image.

snake model, the energy functional is represented as

$$E_{\text{snake}} = \int_0^1 E_{\text{snake}}(v(s)) ds \quad (2)$$

or

$$E_{\text{snake}} = \int_0^1 E_{\text{int}}(v(s)) + E_{\text{image}}(v(s)) + E_{\text{con}}(v(s)) ds. \quad (3)$$

As can be seen from (3), three types of energies influence the snake: internal spline energy (E_{int}), image energy (E_{image}), and external constraint energy (E_{con}). The internal spline energy, represented as

$$E_{\text{int}} = (\alpha(s)|v_s(s)|^2 + \beta(s)|v_{ss}(s)|^2)/2 \quad (4)$$

controls the elasticity of the snake by the first-order term and the rigidity of the snake by the second-order term. The weights $\alpha(s)$ and $\beta(s)$ control the importance of these terms and are chosen according to the characteristics of the contours being sought. Highly curved contours, for example, require a more elastic, less rigid snake ($\alpha > \beta$). Setting the rigidity component (β) to zero would cause the snake to form a corner at an image pixel. The image energy, represented as

$$E_{\text{image}} = w_{\text{line}}E_{\text{line}} + w_{\text{edge}}E_{\text{edge}} + w_{\text{term}}E_{\text{term}} \quad (5)$$

is a weighted combination of line (E_{line}), edge (E_{edge}), and termination (E_{term}) components. The line component is merely the image intensity. This is set depending on whether the snake will be attracted to light lines or dark lines. The edge component attracts snakes to edges in an image by looking for large image gradients. The termination component causes snakes to find the end of line segments and corners. Finally, in the original model, external energy (E_{con}) can be imposed on the snake by an interactive user through use of either a spring or repulsion force. In nearly all applications of snakes, the user is required to initialize the snake by placing it close to the image feature being sought. Under the influence of the combined energy functionals, the snake moves toward the feature automatically.

Snakes include both local and global information, provide user interactive control, incorporate *a priori* knowledge on the properties of the object, and perform segmentation and tracking in a single step. Several variations of the basic snake model can be found in the literature (e.g., [2], [5], [15], [17], [22]).

B. Tracking Using Snakes

A common application for snakes is tracking deformable objects [10], [11]. Snakes are well suited for tracking because they combine object segmentation and tracking into a single step and, once snakes converge on an object, they tend to follow it through sequential frames.

C. Previous Underwater Image Analysis

Underwater imaging typically requires identification of natural and/or manmade features. In an application similar to the subject of this paper, Tang and Stewart describe a pattern recognition system used to classify large numbers of plankton images detected by a towed underwater video system [18]. Although they address plankton classification, their techniques do not process motion and, hence, are not immediately applicable to our problem.

Holland *et al.* use principles of photogrammetry to develop a camera model for measuring nearshore fluid processes, sand bar length scales, foreshore topography, and drifter motions [8]. Their approach appears to be useful in studying underwater geophysical environments.

Conte *et al.* present an automatic system for analysis and interpretation of visual data in submarine pipeline inspection [3]. Their system processes data in real-time to locate the pipe's profile. This application may benefit from an approach that employed active contour models for tracking pipe edges.

III. CONSIDERATION FOR IMPLEMENTATION ON BIOLOGICAL DATA

The underwater video sequences present several unique and challenging issues in developing automated techniques for tracking bioluminescent emissions and identifying the plankton species. Based on the work of Samtaney *et al.* [16], five morphological characteristics are considered: continuation, creation, dissipation, bifurcation, and amalgamation of bioluminescent emissions. Referring to Fig. 4, continuation

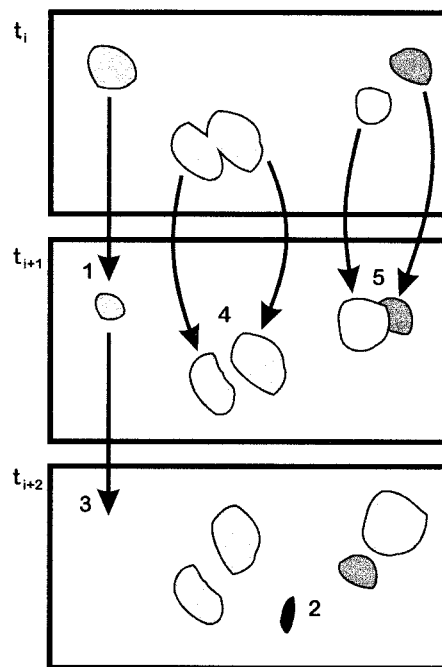


Fig. 4. Morphological characteristics of bioluminescent emissions.

occurs at 1 when an emission continues from time t_i to t_{i+1} with possible rotation, translation, deformation, or change in size. Creation occurs at 2 when a new emission appears. Dissipation occurs at 3 when an existing emission disappears. Bifurcation occurs at 4 when an emission separates into two or more substructures. Finally, amalgamation occurs at 5 when two (or more) emissions appear to merge due to occlusion. Each of these characteristics is exemplified in the video sequences shown in Figs. 5–8.

At first glance, the video sequences would appear to be relatively simple—white blobs segmented against a dark background. However, a closer inspection reveals the unique and dynamic evolution of the emission patterns. Each sequence locates a specific plankton organism so that its emission can be followed. Notice that there are two categories of the emission: luminescence contained within the organism (as in Figs. 5–7) and luminescence secreted from the organism (as in Fig. 8).

Fig. 5 shows a dinoflagellate (*Protoperdinium sp.*), inside the square, with an emission characterized by a short pulse, less than 3 s. This flash is produced as the tiny single-celled organism enters a vortex which draws it through a gap in the transect screen. In this sequence, the organism turns on just after (a), reaches peak luminescence in (b), proceeds through the screen in (c) with a slight lateral shift, and dissipates in the next frame (not shown).

Fig. 6 displays a larger organism called an euphausiid (*Meganctiphanes norvegica*), inside the triangle, whose emission is characterized by a prolonged flash, typically greater than 5-s duration. Since these organisms are too large to pass through the transect screen, they are carried along and subsequently continue to produce flashes in the same location. These repeated flashes should be recognized as the same pattern, and not as the creation of a new emission. The identified organism flashes on in (a), reaches peak luminescence in (b),

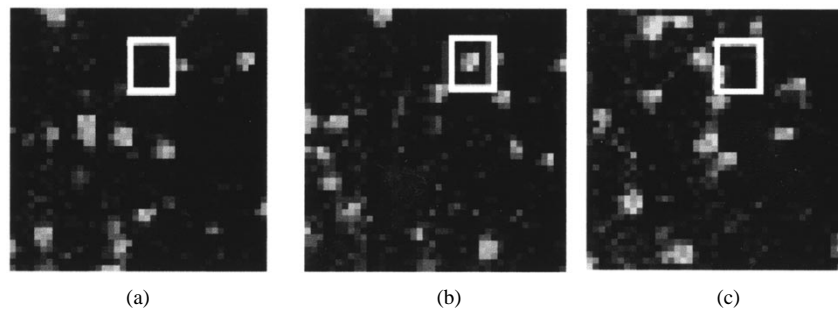


Fig. 5. Sequence showing bioluminescence emission of dinoflagellate. (a) 00:00:13:07. (b) 00:00:13:13. (c) 00:00:15:20.

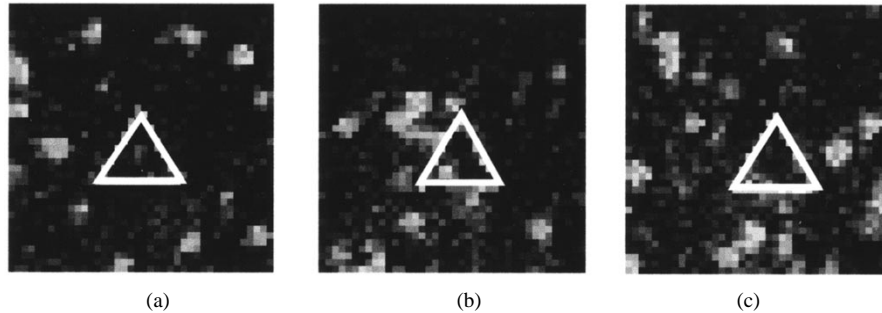


Fig. 6. Sequence showing bioluminescence emission of euphausiid. (a) 00:00:12:23. (b) 00:00:13:16. (c) 00:00:18:20.

and dissipates in (c). The size and intensity of its flash may be slightly greater than that of the dinoflagellate and, as can be noted from the frame count, it is much more persistent.

Fig. 7 shows the pattern of a siphonophore (*Nanomia cara*), inside the rectangle, which is actually a colony of organisms. A siphonophore is difficult to detect since it has a lower intensity; however, once it is detected, it can be easily distinguished by its linear shape and long flash (greater than 10-s duration). In this sequence, the emission becomes faintly visible in (a), reaches peak luminescence in (b), and continues to scintillate for about 30 s until it dissipates. Due to its lower intensity, the siphonophore will not be included in the identification process.

The final sequence, Fig. 8, displays the pattern of a copepod (*Metridia lucens*) inside the box. The copepod commences its appearance in (a) with a size and intensity similar to a dinoflagellate or euphausiid. Its behavior is unique in that its luminescence grows, expanding to more than four times its original size two frames later in (b), and reaches maximum size just five frames after that in (c). After the peak is reached, the diffuse cloud-like shape tends to bifurcate and move across the transect screen as shown in (d)–(f) until it dissipates (not shown). When bifurcation occurs, each part must be recognized as belonging to a common emission, not as a new emission. To further complicate the processing, luminescence from any of the aforementioned organisms may amalgamate in time or space.

Due to the extremely low photon flux of the bioluminescence (10^{11} photons/s or approximately 0.1 mW at the peak of a dinoflagellate flash) and the microscopic size of the plankton, recorded sequences can only be made using an ISIT video camera. The ISIT camera amplifies the signal, thereby allowing even small amounts of light to enlarge (bloom) against a dark background. The narrow dynamic range of the

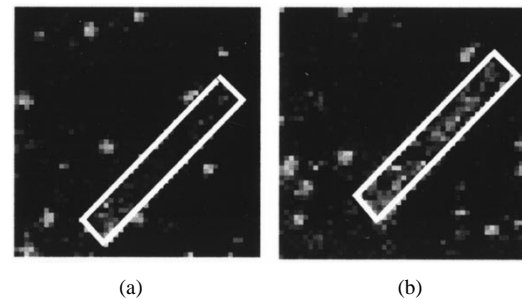


Fig. 7. Sequence showing bioluminescence emission of siphonophore. (a) 00:00:13:07. (b) 00:00:15:11.

ISIT affects the data by easily saturating the intensity levels, hence reducing the number of gray levels. Because of this, complex emission characteristics (or patterns) of each species observed in the laboratory under a microscope cannot be used to identify the plankton; instead, evidence is dependent on the ISIT camera's kinetics. This means the size and duration of the emission will provide more useful information during identification than the intensity levels.

IV. METHODS

In this technique, images in the video sequence are processed sequentially, as shown in Fig. 9. Each new frame from the input data set is processed and the results are integrated into a tracking algorithm. The snake model is used for low-level interaction with image forces. The snake's elasticity component is well suited for segmenting the flexible shapes of the emissions (similar to the biological shapes described by Carlbom *et al.* [1]) and the snakes facilitate tracking. Once the snake converges on an image contour, it takes little time and processing to track contour movements over

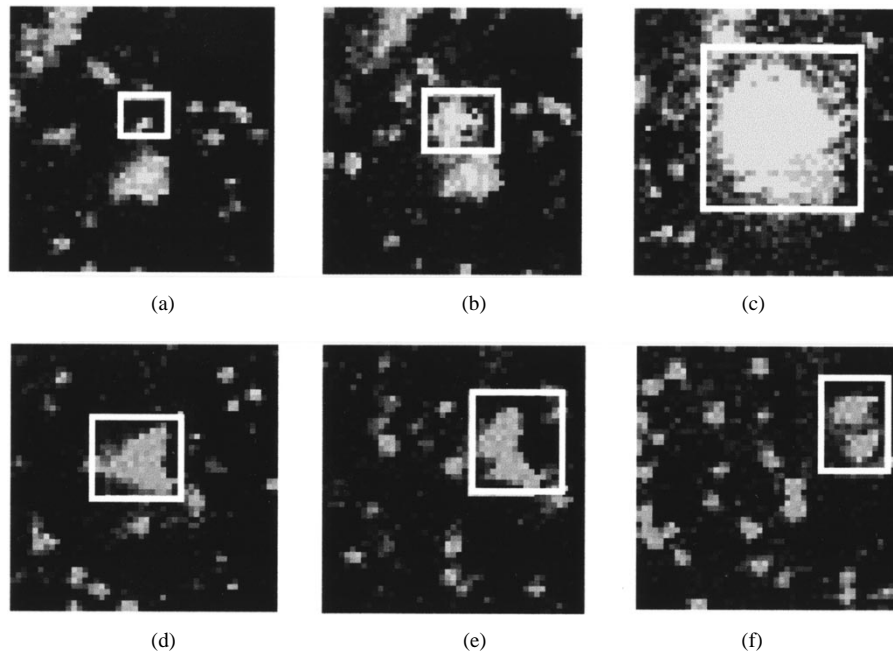


Fig. 8. Sequence showing bioluminescence emission of copepod. (a) 00:00:23:13. (b) 00:00:23:15. (c) 00:00:23:20. (d) 00:00:24:13. (e) 00:00:24:26. (f) 00:00:25:13.

successive frames, especially when sampling at video rates where movements from frame to frame are small. The snakes used in this implementation are made as small as possible in an attempt to reduce tangling problems that occur when a snake bridges the gap between two or more objects.

Unlike typical applications, these snakes are automatically initialized on the image and, rather than permanently marking or following an object (e.g., to seek and track moving lips, pumping heart, etc.) throughout the entire sequence, these snakes have on and off dynamics. New snakes are added to old (existing) snakes in each input frame to locate new emissions, and old snakes are removed from these frames as the emission dissipates. A simplistic method is employed to group overlapping snakes so that the emission boundaries can be located. This approach is computationally less expensive than methods which change the structure of the snake, such as shrinking, growing, and combining contours [14]. Energy minimization is accomplished by calculus of variations methods used in the original snake model. A hierarchical approach is used to maintain object continuity and extract information such as coordinate positions, duration, length, area, peak intensity information, and number of snakes. In this approach, high-level structures having no interaction with the image forces are used to extract the information. Once this information has been collected for the input sequence, each of the located objects can be mapped to a particular plankton species. Details of the segmentation, labeling, tracking, and identification are provided in the following sections.

A. Segmentation

The first step in processing the image is to segment the bioluminescent flash emissions from noise and background. The steps of segmentation are summarized in Fig. 10. In this approach, segmentation is accomplished by cropping and

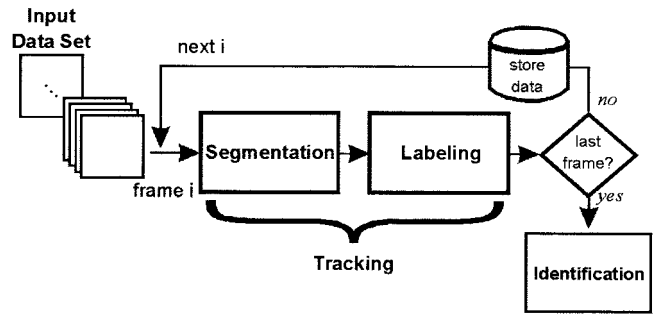


Fig. 9. Steps in processing recorded video sequences.

filtering the 512×512 input image and allowing snakelets to locate the boundaries of the areas of interest. The 256×256 result shown in Fig. 11 demonstrates this process. The region inside the box is used to describe the more detailed steps shown in Fig. 12(a)–(h). Assume that (a) is the first frame in the input data set. Typically, the luminescence is highly contrasted against the dark background of the ocean depths. This means that edges are easily recognizable; however, the gradients are too sharp and narrow and will thus only attract snakelets adjacent to them. To provide a longer range attraction for the snakelets, image gradients are broadened by passing a 3×3 neighborhood dilate morphological operator [6] over the original image to produce the slightly blurred image (b). This blurring also has the advantage of removing small pixel groups (or noise specks) and smoothing jagged edges of larger pixel groups. The dilate morphological operator blurs the image by expanding the maximum intensity pixel in a neighborhood. Next, a 3×3 neighborhood erode morphological operator [6] is passed over the original image to produce the image

1. Get 512x512 input image I_0 .
2. Crop borders / time stamp and sub-sample to get 256x256 image I_1 .
3. Apply 3x3 dilate operator to I_1 to get image I_2 .
4. Apply 3x3 erode operator to I_1 to get image I_3 .
5. Subtract I_3 from I_2 to get edge image I_4 .
6. Invert I_4 to get image I_5 .
7. Randomly drop snakelets onto I_5 .
8. Allow snakelets to converge.
9. Apply extermination algorithm.
10. Store snakelet positions in SAG.

Fig. 10. Algorithm 1. Segmentation.

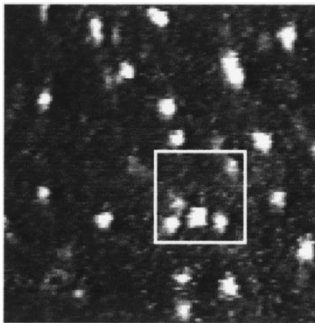


Fig. 11. Recorded image of bioluminescent emissions.

(c). The erode operator reduces the high intensity pixels in a neighborhood. Subtracting the eroded image from the dilated image produces the edge image (d). After inverting this edge image to get (e), thousands of snakelets are dropped in a grid-like manner, with random size and orientation as shown in (f). Each snakelet is composed of 3–6 nodes and a node occupies the space of a pixel. After several iterations of (2), the snakelets begin to settle on the image features as shown in (g). Once a majority of the snakelets converge, an extermination algorithm (summarized in Fig. 13) is applied to each snakelet in the image. The extermination algorithm examines the image gradient on both sides of the snakelet by computing the directional derivative orthogonal to each of its nodes. The derivatives are summed and compared to a threshold value. Low sums indicate that the snakelet has settled on a weak contour, so the snakelet is removed from the image. Snakelets settling on the outlines of the bioluminescent emissions remain as shown in (h). Each of the surviving snakelet node pixel positions are recorded in a snake adjacency graph (SAG) for further processing. Fig. 14 demonstrates the result of the segmentation over the entire image.

B. Labeling

After completing the segmentation, each of the snakelets outlining the bioluminescent emissions are grouped and assigned a label as summarized in Fig. 15. In the first frame of a sequence, these labels are used to initialize the sequence information; however, in all subsequent frames the assigned labels provide temporary frame information. To perform the labeling, each of the emissions is located by examining the surviving snakelets with the assumption that overlapping snakelets com-

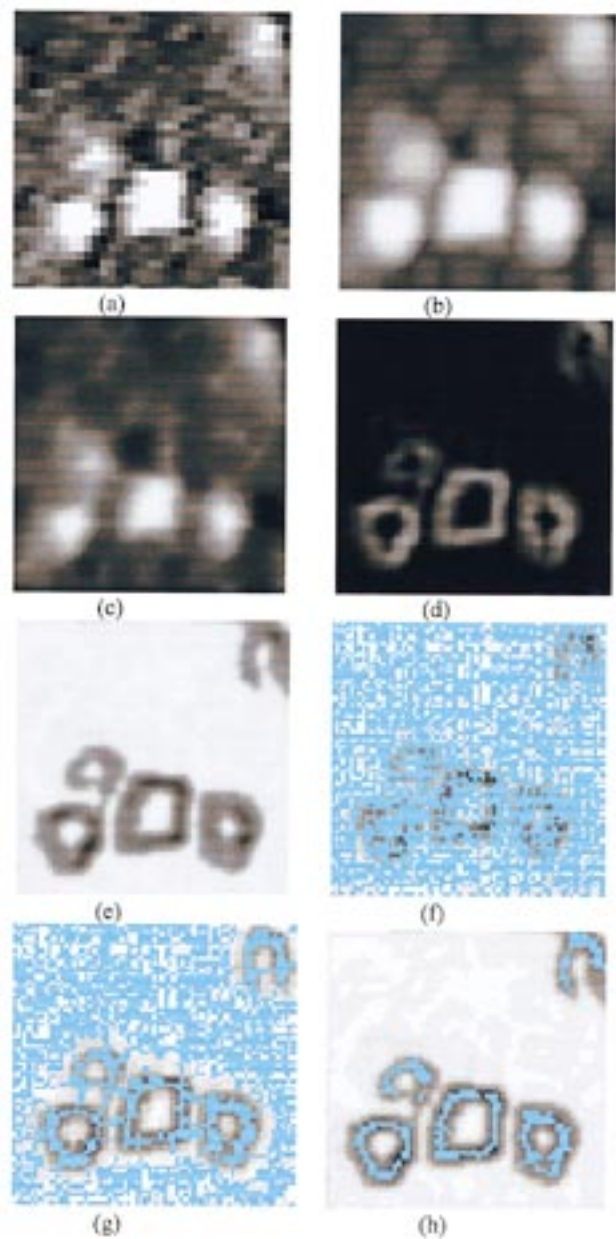


Fig. 12. Example of the steps in segmentation.

bine to surround one or more bioluminescent emissions. The grouping begins by finding the image pixel in the SAG at which the most snakelets intersect. Next, each of the inter-

1. Initialize $left_sum = right_sum = 0$.
2. For each snake node:
 - a. Get orientation of snake at the node from neighbors.
 - b. Add 90 degrees for orthogonal direction.
 - c. Get both left and right orthogonal pixel positions of neighbors.
 - d. Subtract snake node intensity from both left and right side neighbor pixel intensities.
 - e. Add the absolute value of the left side to $left_sum$ and the right side to $right_sum$.
3. Normalize $left_sum$ and $right_sum$ by the total number of nodes in the snake.
4. If both sums are greater than a threshold value then keep the snake.
Otherwise, remove the snake.

Fig. 13. Algorithm 2. Snake extermination.

secting snakelets are traversed so that all connected snakelets are located. The connected snakelets are then moved to a linked-list structure. This process is repeated (e.g., find the image pixel at which the next most snakelets intersect, etc.) for locating all other clusters of snakelets in the image. Once all the clusters are found, each of the snakelet groups in the linked-list are assigned a color and a label $0, 1, 2, \dots, n$, where $n + 1$ is the number of bioluminescent emissions located in that frame. The labeling results from the input image shown in Fig. 11 (not cropped) are shown in Fig. 16.

Although blurring the image during segmentation benefits snake convergence on image features and reduces noise, it also tends to increase the likelihood that two or more bioluminescent emissions will overlap and, thus, become grouped by the snakelets as a single object (not shown in Fig. 16). To correct for this, the area encompassed by each of the emissions in the original image is further examined. Fig. 17 provides an example of this process. Fig. 17(a) shows the resulting snake groups (colored) of the segmentation and labeling overlaid on the edge image. Five groups are circled and labeled using their assigned object number: 0, 1, 9, 19, and 21. A visual inspection reveals that objects 0, 1, and 9 consist of more than one bioluminescent emission. The algorithm for determining this begins by locating the brightest pixel value (intensity) in each emission. Typically, the brightest pixel intensity is found at the center of each emission. (Note that a histogram technique could be applied.) Fig. 17(b) identifies the bright pixel values in the original input image by coloring them orange. Next, the algorithm locates and groups adjacent bright pixels using a two-pass connected component algorithm. Table I lists the information recorded for each of the circled groups. If only one region of bright pixels is found by the algorithm, as is the case with object 21 where the count equals 1, the algorithm concludes that the group consists of a single bioluminescent emission. However, if more than one bright region is found, as is the case with objects 0, 1, 9, and 19, the algorithm tests each region pair to see if there are snakelets separating them. To test for this, image pixels located along a line connecting one region center to the other region center are traversed and each pixel location in the SAG is checked to see if a snakelet node occupies that position. If no snakelets are found (as in object 19), then it is concluded that only one emission is identified. If a snakelet is found, then the number of emissions making

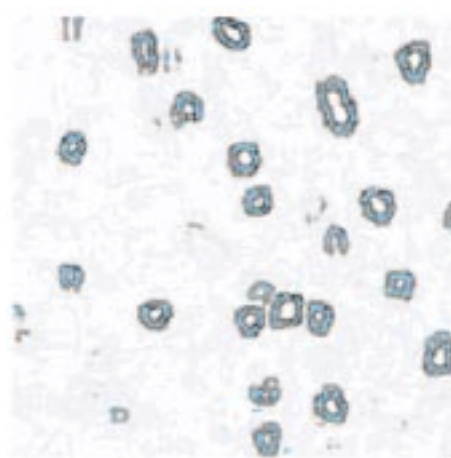


Fig. 14. Segmentation results over entire image.

up the group is incremented. For example, a snake node was found on pixel (87.0, 149.0) separating regions 0 and 1, and on pixel (88.0, 152.0) separating regions 0 and 2 in object group 1, but no snakes were found between regions 1 and 2. With these results, the algorithm concludes that two emissions exist in this group, one composed of region 0 and the other composed of regions 1 and 2. Upon completion, the following data are recorded to a file and stored in a list structure to provide information for object tracking: a list of the group labels found in the frame, the number of bioluminescent emissions making up each group, the number of snakelets comprising the group, the 2-D centroid coordinates of the group, the x and y axis lengths, and the object color (for display only).

C. Tracking

The goal of tracking is to provide a unique sequence identification label to each bioluminescent emission as it moves from frame to frame. In general, the emissions move very little with the exception of the extracellular emissions secreted from copepods. Slight movements are typically caused by water flow through the screen. Nevertheless, tracking begins by initializing each subsequent edge image (I_5 in step 6 of Algorithm 1) with the previous frame's labeled groups. Under the assumption that each of the emissions move only a small displacement from one frame to the next, valid since sampling

1. Locate pixel in SAG with the most intersecting snakelet nodes.
2. Traverse nodes to identify all connecting snakelets.
3. Put connected snakelet information into a linked - list structure.
4. Assign a color and unique label to the linked - list group.
5. Locate pixel with brightest intensity in the group.
6. Apply connected components algorithm to locate adjacent bright pixel regions.
7. Initialize emission count to 1.
8. For each region pair:
 - a. Construct the equation of the line connecting the centers of each region.
 - b. For each pixel location along the line:
 - i. Check pixel location in SAG for snake node.
 - ii. If snake node is found then increment the emission count.
9. Write frame information to file.

Fig. 15. Algorithm 3. Labeling.

occurs at high-speed video rates, the majority of the snakelets in each group will converge on the same group features in the subsequent frame. Segmentation and labeling follow as described in the previous algorithms. Once two consecutive images have been labeled, emissions continuing from one frame to the next are identified as the same object, while new emissions are located and given unique sequence labels. Fig. 18 lists the steps used to accomplish this.

Potential matches are found by comparing the snakelet label numbers in the current group with each of the snakelet label numbers in all groups identified in the previous frame. If any snakelet is found in the previous frame, then the previous frame's group number is added to a list of objects to be considered for matching. If, after checking all the snakelets in a group, there are no matches, a new sequence group number is assigned, indicating a new bioluminescent emission has appeared. If one or more of the current frames' snakelets found matches, four additional conditions are analyzed to determine the best match. Each of the conditions assigns the potential matches a score of 0–100. The scores are summed and the highest score (400 maximum) above a minimum threshold is selected as the best match. The first condition is whether or not the potential match group has already been matched with a previous group in the current frame. If it has been matched, a score of 5 is assigned to the choice; otherwise, a score of 95 is assigned. Typically, repeated matches occur when an emission bifurcates or when two emissions are located so close to each other that they look like the same group. When this occurs, the algorithm tracks each part as the same group number. In the second test condition, the number of snakelets found in each of the previous groups are counted. The value assigned to each potential match is this count divided by the total number of common snakelets, multiplied by 100. Thus, groups with the most snakelet matches receive a higher score. As an example, suppose 80 snakelets in the current group were found in previous group 1, 20 snakelets were found in previous group 2, and 7 snakelets were not found in any previous group. Ignoring the unmatched snakelets, the potential match supporting previous group 1 would add 80 to its current score while the potential match supporting previous

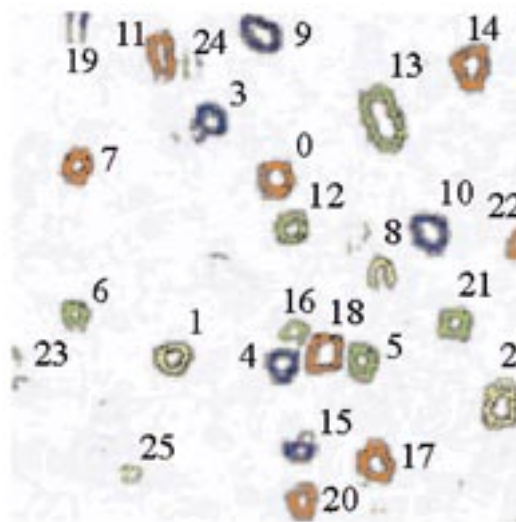


Fig. 16. Labeling results over the entire image.

group 2 would add 20. The third and fourth conditions look at the absolute difference between the x and y center coordinates of the current group and of each potential match group, and assigns a score that is inversely proportional to the difference. Thus, smaller movements are favored (e.g., a difference of zero on an axis receives a score of 100). Once the results are summed, the group number with the highest score above a minimum threshold is selected; if none of the scores are above the threshold, then a new sequence group number is assigned.

An example of tracking results over four input images is shown in Fig. 19. In this figure, each of the identified snake groups is assigned a sequence label and a color. In frame 1, the algorithm identifies five snake groups. These same five groups are matched in frame 2, along with a new emission labeled as 6. Each of the six is identified in frame 3 despite the dynamics of the group size. In frame 4, the number of snakes identifying group 4 falls below the threshold, causing the group to dissipate, while new snakes dropped in this frame identify the creation of group 7. This dynamic behavior is used to map each of the identified snake groups (emissions) to a particular plankton species.

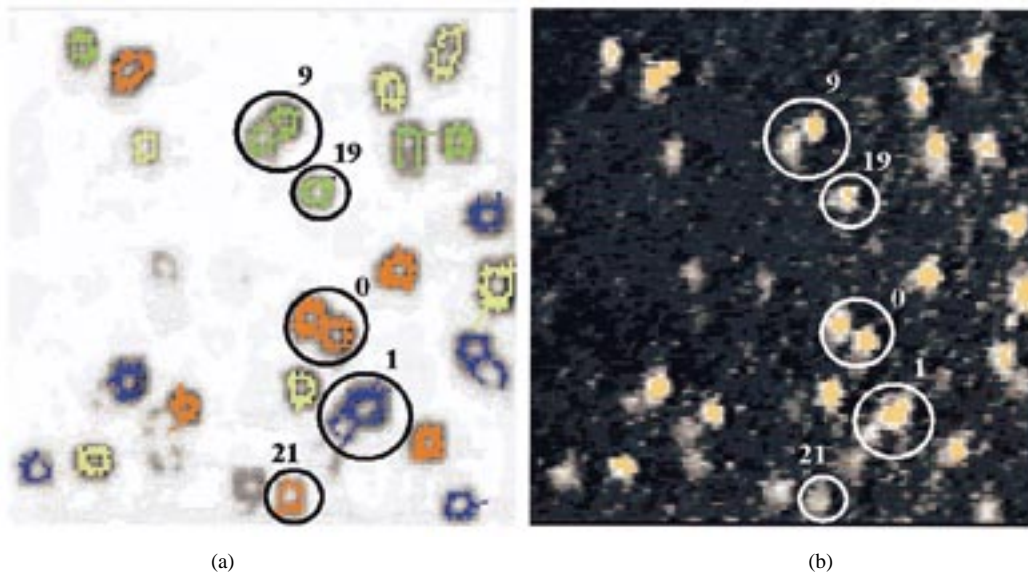


Fig. 17. Determining the number of bioluminescent emissions per group.

For each group in I_n containing snakes s_i :

1. Find all potential matches (pm) in I_{n-1} .
2. For each pm :
 - a. Initialize test score $t = 0$.
 - b. If pm matched previous group then $t = 5$.
Otherwise, $t = 95$.
 - c. Count number of pm snakes found in group (call it c).
 - d. If $c < \text{minimum snake threshold}$ then remove pm ;
Otherwise, $t += (c / \text{total number } s_i) * 100$.
 - e. Compute displacements dx , dy between pm and group.
 - f. If $dx > \text{maximum threshold}$ then $dx = \text{maximum threshold}$.
 - g. If $dy > \text{maximum threshold}$ then $dy = \text{maximum threshold}$.
 - h. Set $dx = 1.0 / (dx + 1.0)$ and $dy = 1.0 / (dy + 1.0)$.
 - i. $t += (dx * 100) + (dy * 100)$.
3. Pick pm with largest t (400 possible) as the match.

Fig. 18. Algorithm 4. Tracking.

TABLE I
CONNECTED COMPONENT ALGORITHM RESULTS

GROUP	REGION	COUNT	X CENTER	Y CENTER	INTENSITY
0	0	16	84.5	173.0	255
	1	14	77.5	176.5	255
1	0	1	85.0	149.0	255
	1	1	91.0	151.0	255
	2	24	91.5	155.5	255
9	0	2	65.0	221.5	255
	1	14	71.0	226.0	255
19	0	2	79.5	207.0	255
	1	5	79.5	210.0	255
21	0	1	36.0	220.0	217

D. Identification

Having tracked each of the bioluminescent emissions through a sequence of frames, the kinetics of each emission are evaluated to identify the plankton. Certainty theory, a technique developed at Stanford University, is applied to

perform the identification with some degree of confidence [13]. In certainty theory, simple rules (R) specify numerical ranges to examine the evidence (E). If a rule is true, a certainty factor (CF) is assigned to each possible hypothesis (H). The CF ranges from -1 to 1 , where 1 means a total belief, -1 means a total disbelief, and 0 means neutral (i.e., no changes to the current CF). The CF value is selected to reflect the confidence in the rule's reliability and may be adjusted to tune the system's performance. Initially, each hypothesis receives a CF value of zero, meaning that there is no information to support or oppose any hypothesis. As each rule is applied, the new CF is calculated for each H as follows:

$$CF = \left\{ \begin{array}{ll} x + y - x^*y, & \text{if both } x, y \geq 0 \\ \frac{x + y}{1 - \min(|x|, |y|)}, & \text{if } x^*y \leq 0 \\ x + y + x^*y, & \text{if both } x, y \leq 0 \end{array} \right\} \quad (6)$$

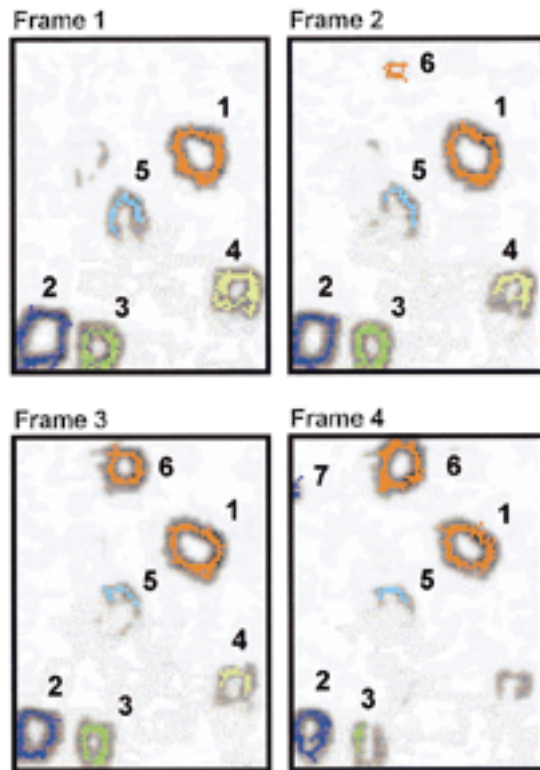


Fig. 19. Example of tracking over four images.

For each emission in the sequence:

1. For each H_i :
 - Initialize $CF=0$ ($1 \leq i \leq 5$).
2. For each rule R_j ($1 \leq j \leq 32$):
 - If rule is true then for each H_i :
 - Compute CF using eq. (6).
3. Select the largest H_i as the plankton species.
4. Store this information to a data file (for the scientist).

Fig. 20. Algorithm 5. Identification.

where x is the current CF for H and y is the CF for the rule being applied. After each of the rules are applied, the hypothesis with the largest CF is selected as the result.

Fig. 20 summarizes the steps involved in identifying the plankton species. During identification, five hypotheses are considered:

- H_1 : dinoflagellate
- H_2 : dinoflagellate-group
- H_3 : euphausiid
- H_4 : copepod
- H_5 : other.

Although H_2 is not a unique species, it is a possible outcome since dinoflagellates that appear to touch or overlap (and become grouped by the snakelets) exhibit different characteristics than those of H_1 . Nine parameters describing the

TABLE II
DOCUMENTED CHARACTERISTICS OF BIOLUMINESCENT EMISSIONS

SPECIES	CHARACTERISTICS
Dinoflagellate	<ol style="list-style-type: none"> 1. Duration < 3 seconds 2. Relatively small emission size 3. Relatively low intensity
Euphausiid	<ol style="list-style-type: none"> 1. Duration > 5 seconds 2. Possibly repeated flashes in same location 3. Relatively small emission size 4. Relatively low intensity
Copepod	<ol style="list-style-type: none"> 1. Begins with relatively small emission size 2. Begins with relatively low intensity 3. Rapidly grows to larger emission size 4. Typically large maximum emission size 5. May split into several parts 6. May move across screen

TABLE III
OBSERVED CHARACTERISTICS OF BIOLUMINESCENT EMISSIONS

CHARACTERISTIC	H_1 (N=499)	H_2 (N=256)	H_3 (N=1)	H_4 (N=10)
Average Duration (frames)	4.62	6.46	151	41.2
Maximum Duration (frames)	20	23	151	103
Minimum Duration (frames)	1	1	151	16
Average Maximum Area (pixels ²)	99.23	123.64	323.51	2276.67
Average Minimum Area (pixels ²)	52.28	49.40	61.93	112.47
Largest Maximum Area (pixels ²)	388.70	858.53	323.51	3195.42
Smallest Maximum Area (pixels ²)	36.91	47.41	323.51	1210.48
Largest Minimum Area (pixels ²)	247.71	305.27	61.93	542.39
Smallest Minimum Area (pixels ²)	1.13	1.81	61.93	8.35
Average Number of Intensity Peaks	1	2.05	1.45	5.9
Maximum Number of Intensity Peaks	1	3	4	9
Minimum Number of Intensity Peaks	1	2	1	3

bioluminescent emission are used as evidence:

- E_1 : duration (frames)
- E_2 : maximum area (pixels²)
- E_3 : minimum area (pixels²)
- E_4 : duration (frames) of maximum area
- E_5 : displacement (pixels) of x -center coordinate from start to stop frame
- E_6 : displacement (pixels) of y -center coordinate from start to stop frame
- E_7 : maximum number of intensity peaks
- E_8 : largest change in area (pixels²) from one frame to the next
- E_9 : maximum number of objects.

The documented behavior and rules of thumb summarized in Table II are used in the formation of each rule [19]–[21]. However, since Table II does not provide numerical boundary values, observed characteristics summarized in Table III are used to construct hypotheses under the assumption that these values provide typical characteristics over a wide range of data sets. Given more observed data, these estimates may be improved. (The value N represents the number of observed cases of the hypothesis.)

By using the information summarized in Tables II and III, the criteria listed in Table IV were constructed to identify the

TABLE IV
CRITERIA FOR TAXONOMIC IDENTIFICATION OF PLANKTON

R _i	E _i	IMPORTANCE	RANGE	H ₁ CF	H ₂ CF	H ₃ CF	H ₄ CF	H ₅ CF
1	1	0.98	(0..16)	0.49	0.49	-0.90	-0.90	0.00
2	1	0.99	[16..25)	0.33	0.33	-0.90	0.33	0.00
3	1	0.60	[25..40)	-0.90	0.00	0.00	0.60	0.00
4	1	0.98	[40..∞)	-0.90	0.00	0.49	0.49	0.00
5	2	0.99	(-∞..400)	0.33	0.33	0.33	-0.90	0.00
6	2	0.70	[400..1000)	-0.90	0.70	-0.90	-0.90	0.00
7	2	0.20	[1000..3500)	-0.90	0.00	-0.90	0.20	0.00
8	2	1.00	[3500..∞)	0.00	0.00	0.00	0.00	1.00
9	3	0.72	(-∞..350)	0.18	0.18	0.18	0.18	0.00
10	3	0.30	[350..3500)	0.00	0.00	0.00	0.30	0.00
11	3	1.00	[3500..∞)	0.00	0.00	0.00	0.00	1.00
12	4	0.99	(-∞..3)	0.33	0.33	0.33	0.00	0.00
13	4	0.60	[3..∞)	-0.30	0.30	-0.30	0.30	0.00
14	5	0.60	(-15..15)	0.15	0.15	0.15	0.15	0.00
15	5	0.60	[-40..-15]	0.00	0.30	0.00	0.30	0.00
16	5	0.60	[15..40)	0.00	0.30	0.00	0.30	0.00
17	5	1.00	(-∞..-40],[40..∞)	0.00	0.00	0.00	0.00	1.00
18	6	0.60	(-15..15)	0.15	0.15	0.15	0.15	0.00
19	6	0.60	(-25..-15]	0.00	0.30	0.00	0.30	0.00
20	6	0.60	(-40..-25]	0.00	0.60	0.00	0.00	0.00
21	6	0.60	[15..25)	0.00	0.30	0.00	0.30	0.00
22	6	0.60	[25..40)	0.00	0.60	0.00	0.00	0.00
23	6	1.00	(-∞..-40],[40..∞)	0.00	0.00	0.00	0.00	1.00
24	7	0.98	[1]	0.49	-0.90	0.49	-0.90	0.00
25	7	0.69	[2]	0.23	0.23	0.23	0.00	0.00
26	7	0.70	(2..10)	-0.10	0.35	-0.10	0.35	0.00
27	7	1.00	[10..∞)	0.00	0.00	0.00	0.00	1.00
28	8	0.78	(-∞..500)	0.26	0.26	0.26	-0.70	0.00
29	8	0.80	[500..∞)	-0.70	0.40	-0.70	0.40	0.00
30	9	0.98	[1]	0.49	-0.98	0.49	-0.90	0.00
31	9	0.70	(1..∞)	-0.90	0.35	0.00	0.35	0.00

plankton species with some measure of confidence. Column one (R_i) of the table lists the rule numbers (1–31). The number of rules is determined by the number of mutually exclusive boundary cases for the evidence, as shown in column two (E_i). Each of the boundary cases for the evidence is grouped together (delineated by solid horizontal lines). (Note that because the boundary conditions are mutually exclusive, only one condition for each piece of evidence will be satisfied when applying Algorithm 5.) The third column, “IMPORTANCE,” is a value 0.0–1.0 indicating how much “weight” the entire piece of evidence should be given. The larger the number, the more important the evidence (e.g., a value of 1.0 means that this evidence alone can be used for identification). Negative weight values can be chosen arbitrarily to detract from supporting a hypothesis (the evidence does not support this hypothesis). The positive CF values in columns five through nine (those assigned to each of the five hypotheses) must add up to the weight value. The selection of the CF values is somewhat *ad hoc*. Initially, best estimates were assigned based on the rule’s reliability. These estimates were later adjusted to produce improved results over the data set. A more accurate means of selecting the CF would be to isolate a single species through a data sequence, apply the rules, and adjust the CF until the expected result is produced. This procedure would be repeated for each of the other species until all CF values are determined. As each of these rules are applied to a plankton group, new CF measures supporting a particular hypothesis monotonically increase just as one would expect for combining evidence.

Note that if a piece of evidence supports the “other” category (H₅ CF= 1.0), the remaining hypotheses are not negated so that the next closest hypothesis can be determined. This may be useful for adjusting the boundary values in Table III. Finally, the fourth column, “RANGE,” numerically bounds the evidence. For example, the bioluminescent emissions duration evidence (E₁) has been separated into the categories: 1–15, 16–24, 25–29, and 40–infinity frames. In the 1–15 category, equal weight is given to H₁ and H₂ because the organisms tend to have short emission duration times; however, negative weights are given to H₃ and H₄ since these organisms produce long-lasting emissions. Although the boundary conditions of the 31 rules are based on the observed characteristics, the values may be better tuned by applying other data sets. Note that, since information was collected from only one euphausiid, boundary values of the dinoflagellate were used with the exception of a longer duration and a slightly larger size (as would be expected).

This completes the description of the methods used in the segmentation, labeling, tracking, and identification of the plankton based on the bioluminescent emission kinetics. Next, results of these techniques are summarized as applied to various data sets.

V. RESULTS

The program results of the described technique are presented in three sections. The first section compares the automatic count of the number of dinoflagellates found in a sequence

TABLE V
ALGORITHM PROCESSING TIME

PROGRAM TASK	TIME (MINUTES)	% TOTAL TIME
Initialize snakes	1.0	4.5
Minimize snakes	2.5	11.4
Exterminate snakes	14.0	63.6
Group snakes	4.0	18.2
Other	0.5	2.3

of frames to an expert's manual (by hand) count. The second section demonstrates tracking of the organisms over a sequence of frames, and the third section counts and identifies the number of organisms found in a sequence of image frames and compares this to the expert's results. Note that only a short 4-s sequence is evaluated for the counting and identification (second and third sections) due to the length of time required for processing. Each image frame required approximately 22 min of processing time running on an R3000 Silicon Graphics Indigo Elan workstation equipped with 80 Mb of RAM (slow by today's PC standards). Table V lists the program tasks and execution times. Although this is nowhere near real-time processing (30 f/s), multiple processors or parallel digital signal processors (DSP's) might make a real-time application feasible. A software modification using information obtained from the minimization algorithm to determine whether or not a snake has settled on an image feature (rather than applying a separate snake extermination algorithm) could also be implemented to speed up the analysis.

A. Dinoflagellate Counting

Typically, dinoflagellates are not counted because there are too many. To evaluate the results of the program, a short, 3-s portion of a video sequence was examined manually by counting the emissions by hand, and then automatically by running the program. The images used were a 128×128 pixel portion of the originally collected data—cropped to reduce the burden of manually counting each organism. In the manual evaluation, the emissions were first counted on a monitor showing the original video data. To facilitate the counting on video, the image was further divided into four smaller quadrants. In addition, each of the images were printed to paper and then counted. Counting from the hardcopy proved to be easier and more accurate than counting from video (colored pens could be used to cross out new and previously counted emissions and a ruler could be used to measure locations of emissions in one frame to the next). Thus, the hardcopy measurement was used as the baseline for all other comparisons. However, it should be noted that counting from a hardcopy is not feasible time-wise for a typical 4-min segment. The same video sequence was next used as input to the program to automatically count the plankton emissions. Once the program is started, no human interaction is required for the duration of the run. The manual and automatic counting results are summarized in Table VI.

In this evaluation, the value counted using the hardcopy data is 357 emissions (baseline). Using the video data, 374 ± 10 emissions were counted manually, providing an accuracy of

TABLE VI
DINOFLAGELLATE COUNTING RESULTS

METHOD	COUNT	% ACCURACY
Manual from printout	357	100.00 (baseline)
Manual from video	374 ± 10	95.24
	384 (worse case)	92.44
	364 (best case)	98.04
Program	336	94.12

95.24% on the average, 98.04% best case, and 92.44% worse case. The program counted 336 emissions yielding an accuracy of 94.12%; thus, 21 were missed. All in all, each of these counts provides sufficient accuracy.

A closer inspection of the program versus the manually counted results reveals that 10 of the 21 program misses were caused by new emissions appearing in approximately the same location as a currently visible emission. When counting, the expert was able to interpret the new emissions, but with a chance of error. It is not likely that the program can be improved to account for many of these instances without significantly advanced signal processing computation for the following reasons.

- 1) It is not easily discernible when two emissions overlap—some human interpretation is required.
- 2) In some cases, the existing emission is of a lower intensity (fading out), but the program cannot use this information to determine that a new emission has appeared since this is a characteristic used to track and identify euphausiids.
- 3) The size (or area) of the existing emission versus the size of the new emission does not change noticeably, so this information cannot be used.

It may, however, be possible to account for some of the remaining 11 misses. The most common problem in these cases is that some of the overlapping emissions did not get counted. The currently implemented algorithm assumes that overlapping emissions would cause the snakes to converge in a "figure-8" shape where snakes would likely separate each of the joined regions. Since this is not always the case, a closer analysis of the interior regions and outlining shape of each emission may provide more information for a more accurate count.

B. Tracking

During the counting process, the program tracks each of the bioluminescent emissions through the video sequence. To estimate the accuracy of the program results, ten of the emissions in sequence 1 were randomly selected from the first frame and manually tracked through five subsequent frames, similar to the approach used by Kumar and Goldgof [11]. Manual tracking was accomplished by a crude method of estimating the center x and y coordinates of each emission from the printed images using a ruler with a minimum scale of 0.02 in. (A more accurate measurement could be made on the original images using a software measurement package.) Once the manual measurements were made, the values were converted from inches to pixels so they could

TABLE VII
MANUAL VERSUS ALGORITHM TRACKING RESULTS

FRAME	MEAN ERROR	VARIANCE
1	1.908	0.586
2	1.379	0.348
3	1.417	0.467
4	1.472	0.468
5	0.869	0.191

TABLE VIII
COUNTING AND IDENTIFICATION RESULTS

PLANKTON SPECIES	EXPERT COUNT	PROGRAM COUNT
Dinoflagellates (includes dino-groups)(H ₁ ,H ₂)	Not Available	1687
Euphausiids (H ₃)	1	1
Copepods (H ₄)	10	9
Other (H ₅)	0	0

be compared to the pixel coordinates automatically generated by the program (1 pixel = 0.01797 in). The absolute distances between the manually extracted coordinates and those given by the program were computed, then a mean absolute distance and variance was calculated for each frame. The results are summarized in Table VII. Although there appears to be better agreement between methods in the fifth frame, this is probably just coincidental. The data do not appear to be substantially different with the possible exception of two emissions that noticeably reduced in size, possibly making it easier to the center coordinates.

C. Counting and Identification

Most importantly, the program must provide total counts for the number of each bioluminescent plankton species found in the video sequence. Manually, euphausiids, copepods, and most jellies (including siphonophores) are counted by looking at the video in real time and occasionally in slow speed when viewing areas of high impact—but never frame by frame. The euphausiids are checked by fast forwarding through the video. On fast forward, these emissions usually remain visible while everything else blinks off. Copepods are easily recognized by the large emission they give off. To test the program's taxonomic classification, a 4-s video sequence was examined by both the program and an expert. Table VIII summarizes the results.

In Table VIII, the dinoflagellate count includes both the single and the grouped emissions. Although this number cannot be verified, a rough check can be made using the data obtained in Table VI. In sequence 1, a 128 × 128 pixel area was examined for a duration of 3 s accounting for approximately 357 dinoflagellates. On the average, 119 dinoflagellate emissions were counted per second. In this example, four times the area is being examined (256 × 256 pixels) over a period of 4 s. Assuming that the population densities are similar in both sequences, this would account for approximately 1904 dinoflagellates. Thus, the program's count of 1687 seems reasonable. The location of the emission identified as euphausiid was verified by the video data, as was a

TABLE IX
PERCENTAGE OF IDENTIFIED HYPOTHESES IN CF RANGE

CF RANGE	% ID				
	H ₁	H ₂	H ₃	H ₄	H ₅
0.980 - 1.000	0.0	13.20	0.0	0.0	0.0
0.970 - 0.979	65.64	6.74	0.0	22.20	0.0
0.950 - 0.969	31.82	69.67	0.0	66.70	0.0
0.900 - 0.949	1.74	10.11	100.0	11.10	0.0
0.000 - 0.899	0.80	0.28	0.0	0.0	0.0

closer inspection of the emissions identified as copepods. As it turns out, eight of the ten copepods located by the expert were identified properly by the program. Two of the ten copepods were not identified by the program for good reasons.

- 1) One copepod emission was located near the left edge of the image. Although this was visible in the video, the majority of the emission was cropped out of the program's input image. The program did not have enough information to make the proper identification.
- 2) The other copepod emission commenced at time 00:00:23:23, with just 00:00:00:07 time remaining in the sequence—far less than the minimum time duration used for identification. This is also acceptable since discontinuities at the beginning and the end of the data set are likely to be encountered.

There was one copepod identified by the program that was not a real copepod. By looking at the input images and the frame data generated by the program, the falsely identified “copepod” is a combination of two adjacent dinoflagellates and possibly a portion of one of the identified copepods. When the snakelets grouped part of the copepod with the dinoflagellates, the area of the group increased significantly (from 115 to 977, then from 977 to 2091) and the center coordinates shifted noticeably [from (204, 76) to (199, 96)]—both typical conditions of a copepod. It is likely that fine-tuning of both the range boundaries and hypotheses CF's will correct this improper identification. However, further experiments should be conducted to determine whether this situation is a rare occurrence or whether there is a problem inherent in the current implementation that should be addressed. In either case, the results presented in Table VII provide valuable timesaving information for the scientist. Table IX summarizes the certainties associated with each identified hypothesis as a percentage of the total number of identifications. For example, looking at column H₁, the program is 97%–97.9% certain that 65.64% of the total emissions identified as dinoflagellates are accurate, 95%–96.9% certain that 31.82% are accurate, 90%–94.9% certain that 1.74% are accurate, and 0%–89.9% that 0.80% are accurate. None of the identified dinoflagellates fell into the 98%–100% certain range. The CF resulting from the identification (Algorithm 5) is used for determining the “CF RANGE.” Each H_{*i*} column sums to 100.00. Optimally, we would like a high percentage of the selected CF's to be skewed toward the higher confidence ranges. Looking at Table IX, this appears to be the case for the program results, since the majority of the identifications are in the range of 0.90–0.979.

This completes the presentation of the results. The next section discusses some of the problems and areas of improvement encountered during implementation.

VI. DISCUSSION AND FUTURE WORK

After analyzing the results of the described technique using data collected *in situ*, several remaining issues can be discussed concerning algorithm shortcomings and future work.

A. Discussion of Shortcomings

The following summarizes the shortcomings of the technique.

- 1) A new emission may be labeled incorrectly (and thus not be counted) if it appears in close proximity to a dissipating emission where the remaining snakes ($>$ the minimum snake threshold defined in Algorithm 4) migrate to the new object.
- 2) The dilate operator may blur the regions between two adjacent emissions causing the snakelets to merge and possibly result in miscounting of the groups.
- 3) Overlapping emissions can get counted as a single emission when snakelets do not separate the intensity peaks.
- 4) When a copepod emission grows in size, other adjacent emissions may get merged with the copepod and miscounted.
- 5) Tracking errors can occur when two or more labeled emission groups combine and become labeled as a single group.
- 6) Plankton may be identified incorrectly if their emission appears near the beginning or end of a sequence where there are not enough data available to correctly identify the species, or if their emission appears near the edges of the frame where cropping occurs.
- 7) Plankton may be identified incorrectly when multiple emissions combine to have similar characteristics of another species (e.g., a dinoflagellate group that looks like a copepod).

B. Future Work

The following additions would aid in making the technique a valuable scientific research tool.

- 1) Apply additional methods to examine merged emissions as identified by dinoflagellate groups. Rather than simply examining the peak intensity pixels of each emission, a histogram of the intensities might prove useful for determining the perimeter of individual emissions which could improve tracking, counting, and area estimation.
- 2) Allow the user to adjust program thresholds since varying populations and/or camera systems may require different settings. One example may be in the detection of the dim and persistent colonies of organisms making up a siphonophore. A two-pass algorithm could be applied which adjusts the dc levels for improved edge detection.
- 3) Apply a supervised statistical or neural network classifier algorithm rather than the current method of identification in which classifier parameters must be selected through trial and error each time the camera settings or surrounding environment changes. Techniques such as these

would also provide a way of updating the kinematic characteristics and identification rules in the program's database as new plankton species are encountered.

VII. CONCLUSION

The research described in this paper demonstrated a novel automated approach to quantifying, tracking, and identifying bioluminescent plankton. Algorithms were described to perform segmentation, labeling, and tracking of the bioluminescent emissions using active contour models, and a method was presented for taxonomic identification of the plankton species using certainty theory. These techniques were tested with data collected *in situ* and results were presented which achieved accuracy close to expert level for counting and identifying the plankton. Using this automated approach, scientists will have the ability to study and characterize the spatial and temporal relationships of bioluminescent plankton in their 3-D underwater environment. Furthermore, methods such as these can be generalized to other video analysis tasks in underwater imagery.

ACKNOWLEDGMENT

The authors wish to thank A. M. Clark, S. D. Lang, and F. M. Caimi for technical advice and support, T. Frank for manual data analysis and editorial suggestions, and D. Terzopoulos for providing preliminary snake code.

REFERENCES

- [1] I. Carlom, D. Terzopoulos, and K. Harris, "Computer-assisted registration, segmentation, and 3D reconstruction from images of neuronal tissue sections," *IEEE Trans. Med. Imag.*, vol. 13, pp. 351–362, June 1994.
- [2] J. M. Chassery and Y. Elomary, "Deformable models in a multiresolution environment," Tech. Rep., 1994.
- [3] G. Conte, S. Zanolli, A. M. Perdon, G. Tascini, and P. Zingaretti, "Automatic analysis of visual data in submarine pipeline," in *Proc. IEEE OCEANS'96*, Fort Lauderdale, FL, Sept. 1996, pp. 1213–1219.
- [4] Y. L. Fok, C. K. Chan, and R. T. Chin, "Automated analysis of nerve-cell images using active contour models," *IEEE Trans. Med. Imag.*, vol. 15, pp. 353–368, June 1996.
- [5] S. R. Gunn and M. S. Nixon, "A robust snake implementation; A dual active contour," *IEEE Trans. Pattern Anal. Machine Intell.*, vol. 19, pp. 63–68, Jan. 1997.
- [6] R. M. Haralick and L. G. Shapiro, *Computational Robot Vision*. Reading, MA: Addison Wesley, 1992, vol. 1, pp. 158–159.
- [7] P. J. Herring, "Bioluminescence in decapod crustacea," *J. Mar. Biol. Ass.*, UK, vol. 56, pp. 1029–1047, 1976.
- [8] K. T. Holland, R. A. Holman, T. C. Lippmann, and J. Stanley, "Practical use of video imagery in nearshore oceanographic field studies," *IEEE J. Oceanic Eng.*, vol. 22, pp. 81–92, Jan. 1997.
- [9] M. Kass, A. Witkin, and D. Terzopoulos, "Snakes: Active contour models," in *Proc. ICCV*, 1987, pp. 259–268.
- [10] D. L. Kraitchman, A. A. Young, C. N. Chang, and L. Axel, "Semi-automatic tracking of myocardial motion in MR tagged images," *IEEE Trans. Med. Imag.*, vol. 14, pp. 422–433, Sept. 1995.
- [11] Kumar and S. D. Goldgof, "Automatic tracking of SPAMM grid and the estimation of deformation parameters from cardiac MR images," *IEEE Trans. Med. Imag.*, vol. 13, pp. 122–132, Mar. 1994.
- [12] Y. H. Kwon and N. da Vitoria Lobo, "Age classification from facial images," in *Proc. IEEE CVPR*, Seattle, WA, June 1994, pp. 762–767.
- [13] G. F. Luger and W. A. Stubblefield, *Artificial Intelligence and the Design of Expert Systems*. Redwood City, CA: Benjamin/Cummings, 1989.
- [14] T. McInerney and D. Terzopoulos, "Topographically adaptable snakes," in *Proc. IEEE Int. Conf. on Computer Vision*, Cambridge, MA, June 1995, pp. 840–845.
- [15] W. Neuenschwander, P. Fau, G. Szekely, and O. Kubler, "Initializing snakes," in *Proc. IEEE CVPR*, 1994, pp. 658–663.

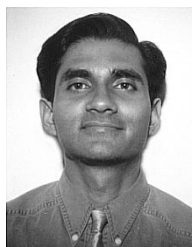
- [16] R. Samtaney, D. Silver, N. Zabusky, and J. Cao, "Visualizing features and tracking their evolution," *IEEE Trans. Comput.*, vol. 27, pp. 20–27, July 1994.
- [17] L. H. Staib and J. S. Duncan, "Boundary finding with parametrically deformable models," *IEEE Trans. Pattern Anal. Machine Intell.*, vol. 14, pp. 1061–1075, Nov. 1992.
- [18] X. Tang and W. K. Stewart, "Plankton image classification using novel parallel-training learning vector quantization network," in *Proc. IEEE/MTS OCEANS'96*, Fort Lauderdale, FL, Sept. 1996.
- [19] E. A. Widder, S. Bernstein, D. Bracher, J. F. Case, K. R. Reisenbichler, J. J. Torres, and B. H. Robison, "Bioluminescence in monterey submarine canyon: Image analysis of video recordings from a midwater submersible," *Marine Biol.*, vol. 100, pp. 541–551, 1989.
- [20] E. A. Widder, C. H. Greene, and M. J. Youngbluth, "Bioluminescence of sound-scattering layers in the gulf of Maine," *J. Plankton Res.*, vol. 14, no. 11, pp. 1607–1624, 1992.
- [21] E. A. Widder, "In situ video recordings of bioluminescence in the ostracod, *Conchoecia elegans*, and co-occurring bioluminescent plankton in the gulf of Maine," in *Proc. Int. Symp. Bioluminescence and Chemiluminescence*, Sussex, U.K., 1997.
- [22] D. J. Williams and M. Shah, "A fast algorithm for active contours and curvature estimation," *Computer Vision, Graphics, Image Processing*, vol. 55, pp. 14–26, 1992.



Donna M. Kocak received the B.Sc. and M.Sc. degrees in computer science from the University of Central Florida, Orlando, in 1989 and 1997, respectively.

She joined the Engineering Division of Harbor Branch Oceanographic Institution, Fort Pierce, FL, in 1990, where she is now a Software Engineer. Her areas of specialization include computer vision, computer graphics, and instrumentation software development.

Ms. Kocak is a member of the IEEE Computer Society, the Society of Photo-Optical Instrumentation Engineers, the Marine Technology Society, and Upsilon Pi Epsilon Honor Society for the Computing Sciences.



Niels da Vitoria Lobo completed the B.Sc. (honors) degree at Dalhousie University, Canada, in 1982, and the M.Sc. and Ph.D. degrees at the University of Toronto, Toronto, ON, Canada, in 1985 and 1992, respectively.

He is currently an Associate Professor at the University of Central Florida, Orlando, in the School of Computer Science. His research interests are in computer vision and in physical modeling for computer graphics. His funding sources include the National Science Foundation and the US Department of Defense. He has several patents, numerous publications, and currently supervises a number of graduate students.

Dr. da Vitoria Lobo is a member of the IEEE Computer Society.



Edith A. Widder received the B.Sc. degree (*magna cum laude*) in biology from Tufts University, Medford, MA, in 1973, and the M.Sc. degree in biochemistry and the Ph.D. degree in neurobiology from the University of California at Santa Barbara in 1977 and 1982, respectively.

She joined Harbor Branch Oceanographic Institution, Fort Pierce, FL, in 1989, where she is now a Senior Scientist and Director of the Bioluminescence Department. Her research has involved the development of a number of instrument systems, including the HIDEX-BP on which she co-holds the patent and which is now the standard in the U.S. Navy for measuring bioluminescence in the oceans.